The 2016 World Congress on
The 2016 Structures Congress (Structures16)
Jeju Island, Korea, August 28-September 1, 2016

Structural Performance of Pilotis-Wall System without Transfer Girder

*Sung Hyun Kim[1)] , Hong-Gun Park[2)] and Hyeon-Jong Hwang[3)]

[1), 2)] *Department of Architecture & Architectural Engineering, Seoul National University, Seoul 151-744, Korea*

[3)] *College of Civil Engineering, Hunan University, Hunan 410082, China*
[1)] *jangson@snu.ac.kr*

ABSTRACT

In Korean apartments, pilotis-wall frame systems have been frequently used. For cost-effectiveness design, the present study focuses on the removal of the transfer girder in the pilotis-wall systems. On the basis of the capacity design, new pilotis-wall system without the transfer girder was proposed, in which the transfer zone between the pilotis and wall were reinforced with a significant amount of reinforcement bars. To evaluate the structural performance of the proposed system, compression and cyclic loading tests were performed in four wall specimens. All specimens exhibited greater ultimate strength than the design strength and ultimately failed in the wall above the transfer zone.

1. INTRODUCTION

Recently, pilotis-wall frame system in the lower story of Korean apartments has been widely used to provide resting places and to solve the unpleasant surroundings and privacy issues. In the pilotis-wall frame system, the gravity and lateral loads are transferred by the transfer girder between the wall and pilotis. However, the use of the transfer girder causes some problems: 1) over 1.8 m depth of the transfer girder decreases the efficiency of space; and 2) large-sized transfer girder reduces the constructability, which increases the construction period.

In the present study, new pilotis-wall frame system without transfer girders, in which an upper wall was directly connected with pilotis, was developed. On the basis of the capacity design concept, a design method for the proposed system was discussed. To evaluate the structural performance of the proposed system and verify the design method, both the compression loading and cyclic loading tests were performed.

[1)] Graduate Student
[2)] Professor
[3)] Assistant Professor

2. EXPERIMENTAL PROGRAM

2.1 Design Concept

In the case of pilotis-wall system, the gravity and lateral loads from above walls are transferred to pilotis through the transfer zone. In the wall-pilotis connection, stress is concentrated due to the significant decrease of cross-sectional area. Thus, to avoid the premature brittle failure in the connection, the capacity design method based on the actual performance of the structure was used. In the method, each structural member is designed on the basis of the assumed failure mode. Fig. 1 shows two failure modes of the pilotis-wall system. Brittle failure in the connection is not recommended for seismic design of the structure [Fig. 1(a)]. In this study, pilotis and wall in transfer zone were designed to resist the required load greater than the load capacity of the upper wall. As a result, plastic hinge occurs at the upper wall, which causes the ductile failure mode [Fig. 1(b)].

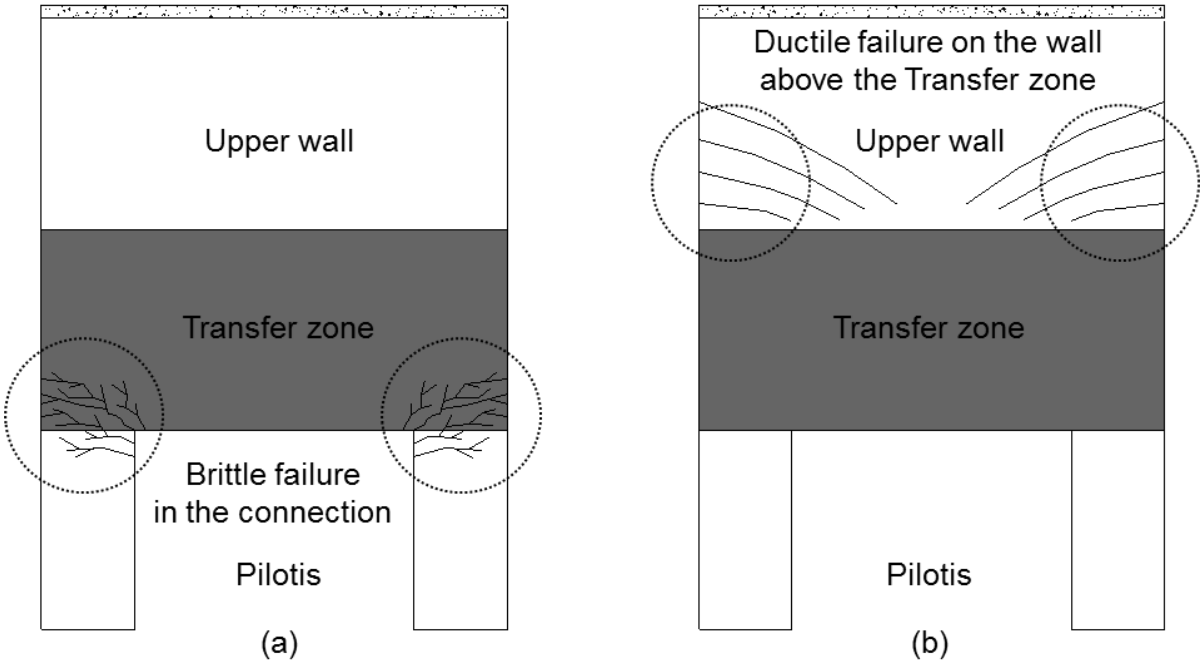

Fig. 1 Failure modes of the pilotis-wall system

2.2 Design Procedure

Fig. 2 shows the two different design methods for the design of the reinforcement. The critical section *bh* was defined as the area where the wall and the pilotis are connected. Thus, the nominal strength of each critical section was calculated by following equation.

$$P_n = 0.85 f_c' bh \tag{1}$$

where f_c' = concrete strength; b = depth of the pilotis; and h = thickness of the wall.

When the compression load and lateral load are applied, two kinds of axial forces occur in the critical section [Fig. 2(a)]: P_g due to the axial compression; and P_v due to the lateral load.

$$P_g = P_u/2 \tag{2}$$

$$P_v = V_u H/L \tag{3}$$

On the basis of the resultant force of the two axial forces P_v and P_g, the design lateral load V_u can be calculated.

$$P_n = P_v + P_g = P_u/2 \ + V_u H/L \tag{4}$$

$$V_u = (P_n - P_u/2)L/H \tag{5}$$

On the other hand, in the critical section of the tension side, the resultant force is developed as a tension force T_{u1}. In order to resist the tension force, the longitudinal reinforcement was placed, and more longitudinal reinforcement were arranged to avoid the premature failure in the transfer zone.

Tensile force T_{u2} in the transfer zone was evaluated by using a strut-tie model.

$$T_{u2} = P_u/4 + V_u \tag{6}$$

For a conservative design, the required lateral reinforcement in this area was increased by 25%.

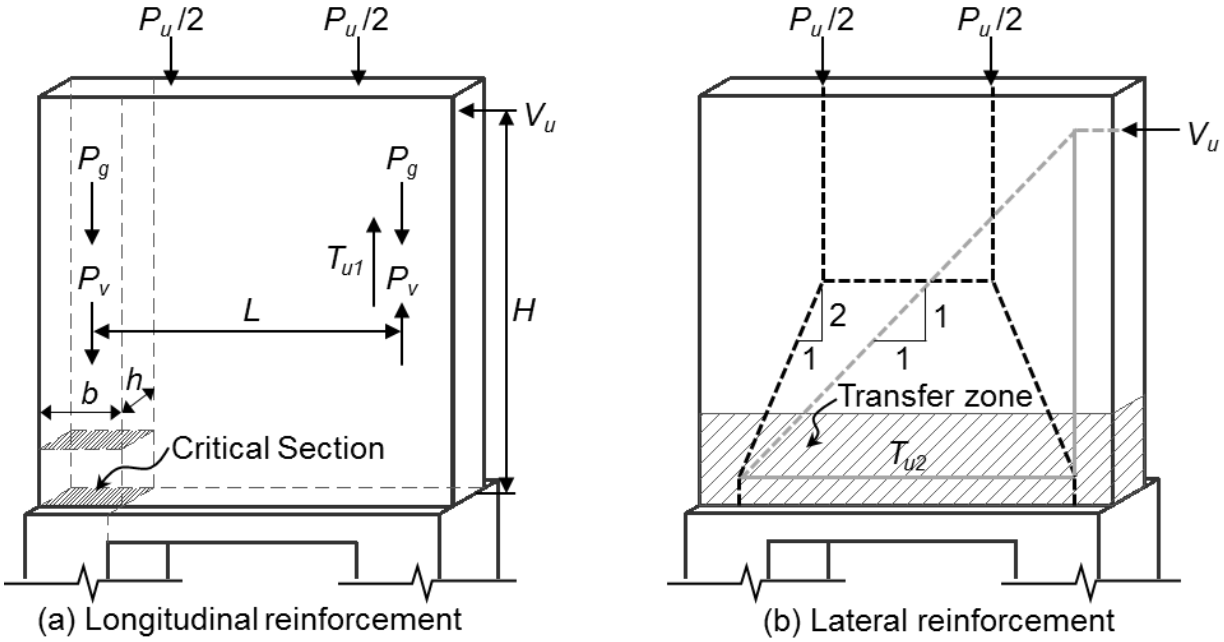

Fig. 2 Design of the reinforcement

2.2 Test Specimens and Setup

Table 1 lists the test parameters of four wall specimens. Three cyclic loading tests were performed on the specimens C1, C2, and C3, and a compression test was performed on the specimen G1. ρ_v = longitudinal reinforcement ratio calculated in the critical section, A_{st} = lateral reinforcements in the transfer zone, P_n = nominal axial capacity of the critical section, P_u = design compression load, and V_u = design lateral load. As main test parameters, parameter1 indicates the contribution ratio of the compressive load to lateral load at the critical section, which evaluates the effect of earthquake load. Parameter2 evaluates the effect of the pilotis depth (360 mm and 450 mm).

Table 1 Test parameters of test specimens

Specimens		ρ_v (%)		A_{st}	P_n (kN)	P_u (kN)	V_u (kN)	Parameter1 *P : V*	Parameter2 $B_{pilotti}$ (mm)
		Wall	Pilotis						
Compression	G1	0.37	2.98	12-D16	3428	3428	-	100 : 0	360(40%)
Cyclic Loading	C1	1.32	2.98	16-D16	3594	1334	801	37 : 63	360(40%)
	C2	3.13	5.38	16-D16	3819	860	1049	23 : 77	360(40%)
	C3	3.05	5.38	18-D16	4284	980	1099	23 : 77	450(50%)

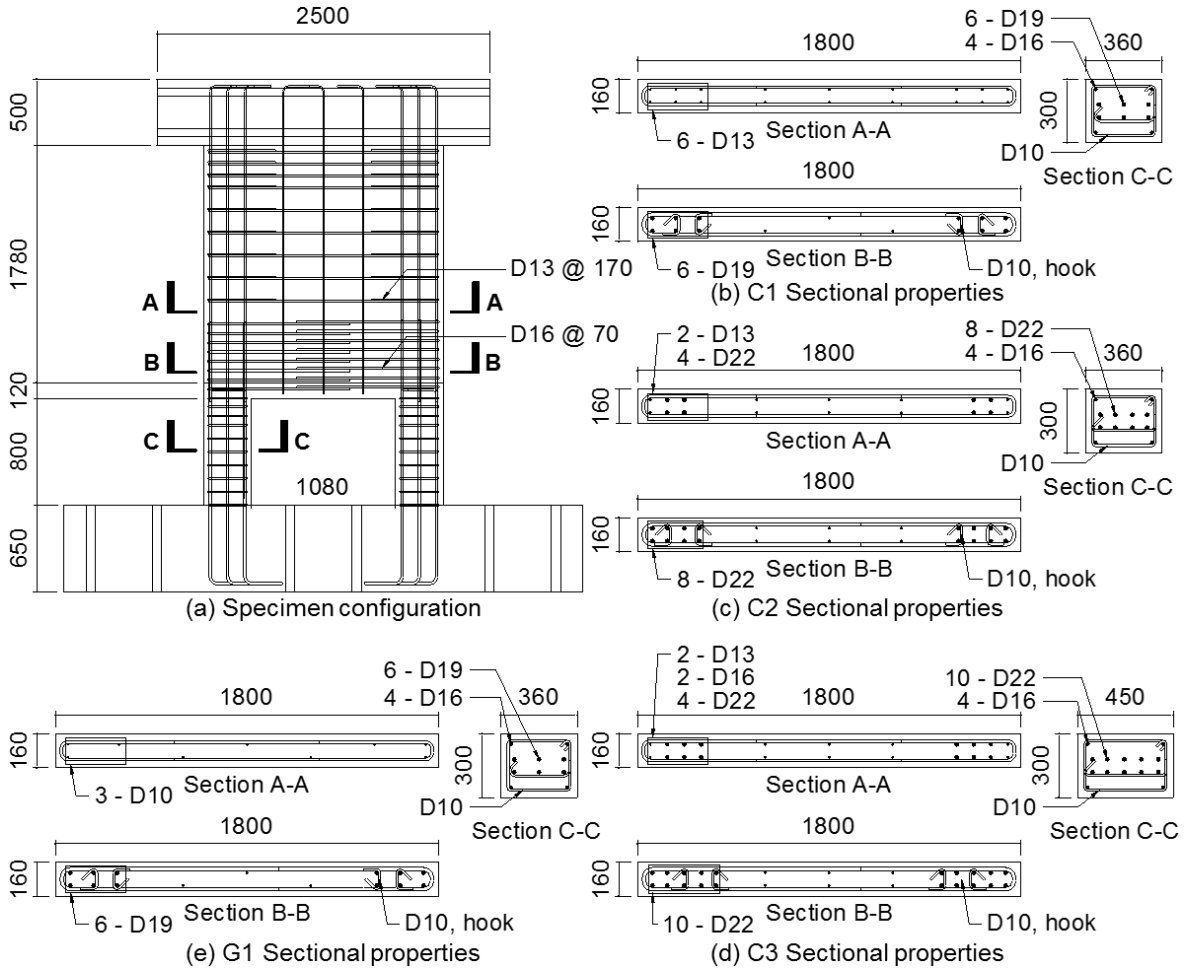

Fig. 3 Dimensions and details of test specimens (mm)

Fig. 3 shows dimensions and details of one-third scaled wall specimens with three stories. Relatively higher amount of longitudinal reinforcements was placed in the transfer zone (section B-B) compared with the upper wall (section A-A). Considering the stress concentration at the critical section, most of the reinforcements were placed at the center of pilotis (section C-C).

Fig. 4 shows the test setups for cyclic loading and compression tests. Cyclic lateral loading was applied to the test specimens subjected to uniform axial load. The cyclic loading protocol was planned according to ACI 374.2R-13 (ACI 2013). Lateral deformation was measured at the center of the loading point. In the case of the compression test, the axial load was applied to the top of the specimen using 10,000kN universal test machine. The net height of the specimen was 2700mm and axial deformation of the specimen was measured at the four corner of the specimen.

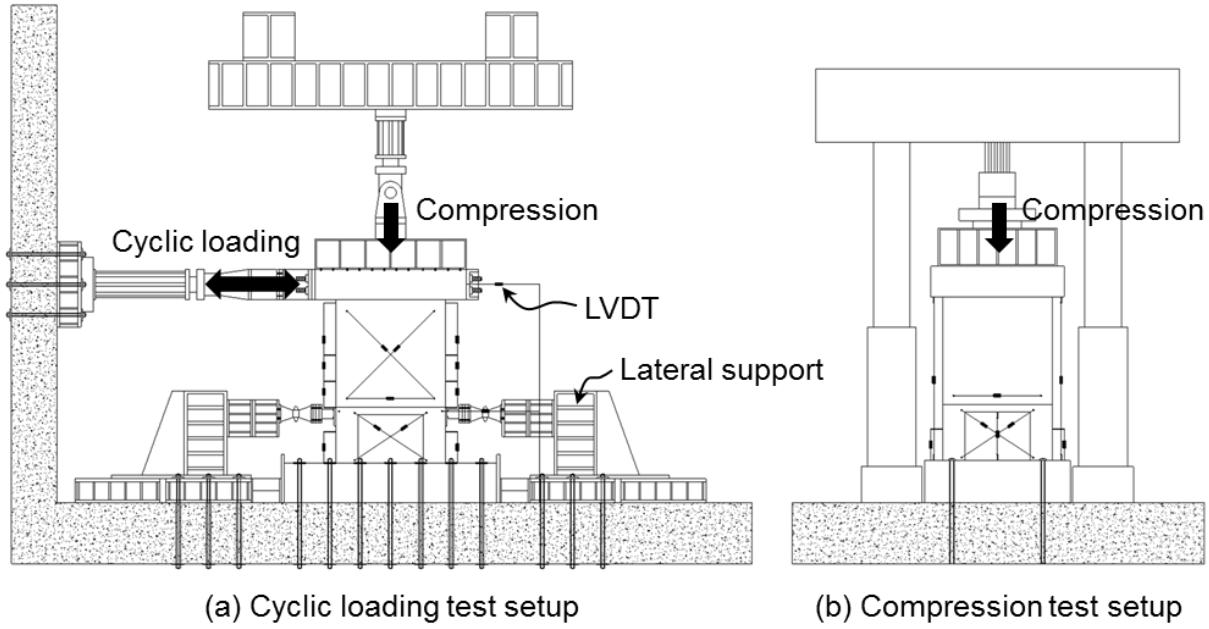

Fig. 4 Test setups

3. TEST RESULTS

3.1. Cyclic loading test

Fig. 5 shows the lateral load – drift ratio relationships. The lateral drift ratio was calculated from the lateral drift at the loading point and net height of the wall (=2150 mm). The peak strengths V_{exp} of all specimens were greater than the design strength V_u. All of the specimens showed ductile behavior after yielding, and concrete crushing occurred at δ = 1.0 to 1.5% in the compression region.

Fig. 6 shows failure modes of the specimens. In specimens C1 and C2, concrete crushing occurred at the height of 400 mm from the bottom face of the wall. Furthermore, buckling of the longitudinal bars was observed. In specimen C3, concrete

crushing occurred at the height of 600 mm from the bottom face of the wall. However, buckling of the re-bars was not found due to the less concrete crushing.

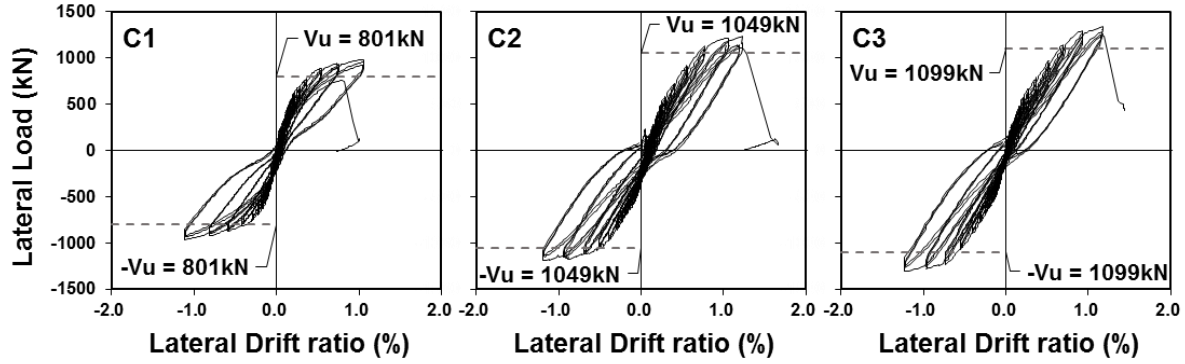

Fig. 5 Lateral load – drift ratio relationships of specimens

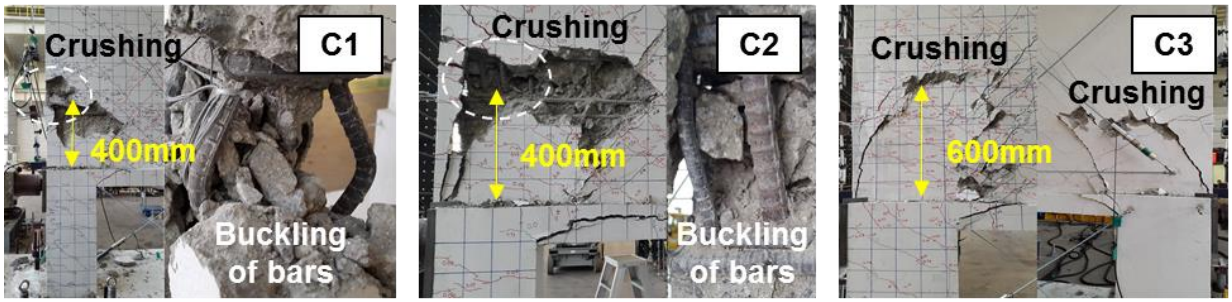

Fig. 6 Failure modes at the end of the tests

Table 2 shows the cyclic loading test results. The yield drift ratio was calculated based on equivalent elasto – plastic energy absorption model (Park 1988). The maximum drift ratio was defined at the failure.

In the case of the specimen C1 which had a greater axial force ratio, the ductility was greater than that of the others due to the greater yield stiffness.

In the case of the specimen C3 which had a larger depth of pilotis, the ductility was less than that of the others. However, C3 exhibited greater ultimate strength than the others.

Table. 2 Summary of cyclic loading test results

Specimen	Test strength		Nominal strength	Yield drift ratio		Maximum drift ratio		Ductility		Yield stiffness
	V_{exp} (kN)		V_u (kN)	δ_y (%)		δ_u (%)		μ (=δu/δy)		K_y (kN/mm)
	Positive	Negative		Positive	Negative	Positive	Negative	Positive	Negative	
C1	979	-961	801	0.44	0.41	1.06	1.12	2.4	2.7	102.3
C2	1231	-1193	1049	0.75	0.43	1.29	1.20	1.7	2.8	76.4
C3	1334	-1310	1099	0.72	0.60	1.44	1.22	2.0	2.1	86.5

Fig. 7 shows the rebar strains. In the pilotis and transfer zone, rebar strains were less than the yield strain [Figs. 7(a) to (c)]. In the upper wall, however, rebar strains exceeded the yield strain as the load increases. This is because the damage is concentrated and the rebar buckling occurred in the upper wall.

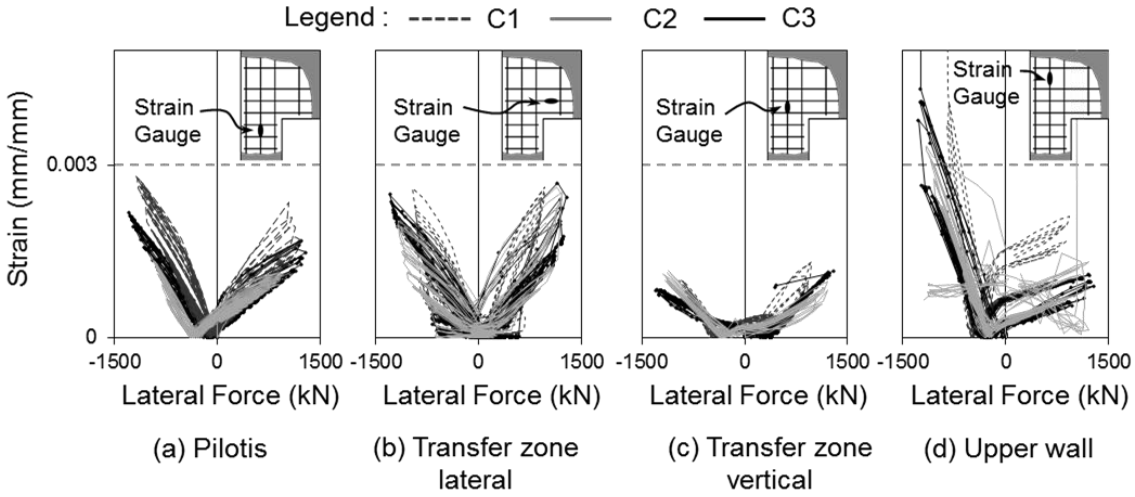

Fig. 7 Rebar strains of the specimens under cyclic loading

3.2. Compression Test

Fig. 8 shows axial load – strain relationship. The axial strain was calculated from the average axial deformation at the four corners and net height of the specimen (=2700 mm). The peak strength P_u was 5414 kN which was 1.44 times the nominal strength P_n = 3748 kN. Concrete crushing occurred at P_{cr} = 5342 kN in the compression region.

Fig. 9 shows damages in the specimen. Concrete crushing occurred at the height of 300mm from the bottom face of the wall. Furthermore, buckling of the longitudinal bars was observed. The damage in the pilotis and transfer zone were limited.

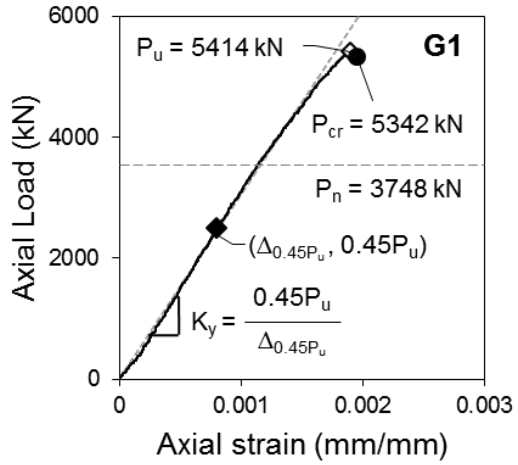

Fig. 8 Axial load – strain relationship

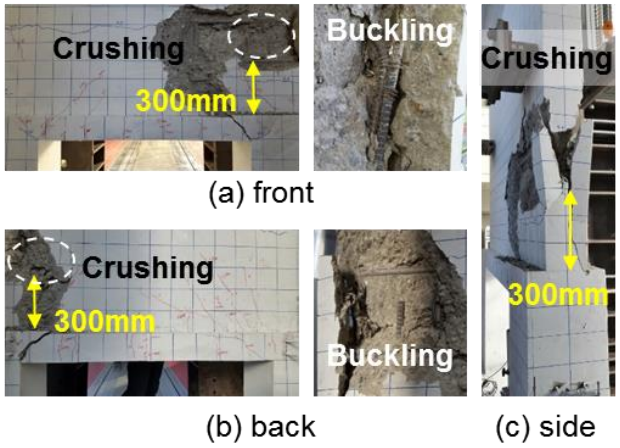

Fig. 9 Damages in specimen G1

Fig. 10 shows the strain variations of the re-bars according to the axial load. In the pilotis and transfer zone, rebar strains were less than the yield strain [Figs. 10(a) to (c)]. In the upper wall, however, rebar strains exceeded the yield strain as the load increases. This is because the damage is concentrated and the rebar buckling occurred in the upper wall.

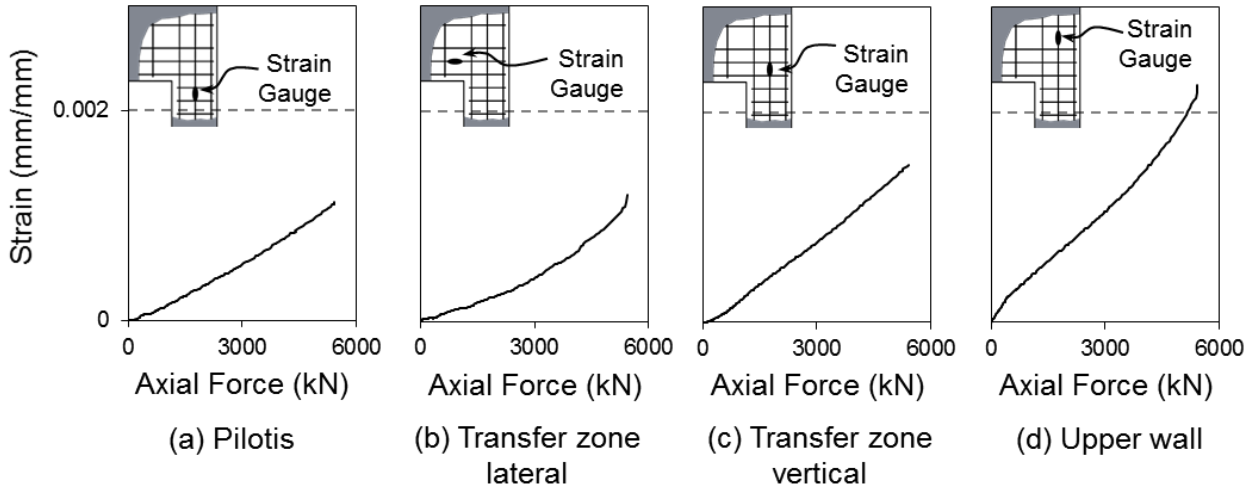

Fig. 10 Rebar strains of the specimens under compression

4. CONCLUSIONS

In the present study, in order to evaluate the structural performance of pilotis-wall frame system without transfer girder, cyclic lateral loading tests and compression test were performed. From the test results, the load carrying capacity, deformation capacity and failure mode of the specimens were investigated. The test results are summarized as follows:

1. In the specimens of the cyclic loading tests, the lateral load-carrying capacities were greater than the nominal strengths. All of the specimens showed ductile behavior after yielding and finally concrete crushing occurred at the height of 400 mm and 600 mm. The external damages in the transfer zone and pilotis were relatively limited. The ductility of the specimens was between 2.0 to 2.7. Rebar strains in the transfer zone and pilotis were less than the yield strain, while the maximum rebar strain in the upper wall was greater than the yield strain.
2. In the specimen of the compression test, the axial load capacity was greater than the nominal strength. Concrete crushing occurred in the compression region at the height of 300 mm from the bottom face of the wall. The external damages in the transfer zone and pilotis were relatively limited. Rebar strain in the transfer zone and pilotis was less than the yield strain, while the maximum rebar strain in the upper wall was greater than the yield strain.
3. These results indicate that, when the transfer zone is designed by the capacity design concept in the pilotis-wall system, brittle failure in the transfer zone and pilotis can be prevented.

REFERENCES

Park, R. (1988), “Ductility evaluation from laboratory and analytical testing”, *In Proceedings of the 9th World Conference on Earthquake Engineering*, Tokyo-Kyoto, Japan (Vol. 8, pp. 605-616).

ACI (2013), “Guide for testing reinforced concrete structural elements under slowly applied simulated seismic loads”, *ACI 374*.